

Crystal Structure and Chemical Characterization of $\text{La}_{0.7}\text{Sr}_{0.3}\text{Mn}_{0.7}\text{Ti}_{0.3-x}\text{Al}_x\text{O}_3$ ($0 \leq x \leq 0.15$) Compounds

I.O. TROYANCHUK^{a,*}, M.V. BUSHINSKY^a, N.V. TERESHKO^a, V.V. FEDOTOVA^a

AND J. PARTYKA^b

^aScientific-Practical Materials Research Center of NAS of Belarus, Str. P. Brovka 19, 220072 Minsk, Belarus

^bLublin University of Technology, Nadbystrzycka 38a, 20-618 Lublin, Poland

Neutron powder diffraction and magnetization measurements have been performed for $\text{La}_{0.7}\text{Sr}_{0.3}\text{Mn}_{0.7}\text{Ti}_{0.3-x}\text{Al}_x\text{O}_3$ ($0 \leq x \leq 0.15$) stoichiometric compounds. Increase of the Al^{3+} content enlarges the Mn^{4+} ions fraction from 0% ($x = 0$) up to around 20% ($x = 0.15$). The $x = 0$ composition around 150 K exhibits a structural transition from the rhombohedral phase to the orthorhombic one whereas the crystal structure of the compounds with $x = 0.1$ and 0.15 remains to be rhombohedral down to 2 K. The substitution of Ti^{4+} by Al^{3+} ions is accompanied by a gradual increase in the bond angle Mn–O–Mn and decrease in the Mn–O bond length which lead to enhancement of the covalent component of the chemical bond. All these compounds exhibit ferromagnetic components below 100 K. Magnetic moments estimated per manganese from the neutron powder diffraction data are found to be around $1.3 \mu_B$ ($x = 0$) and $1.7 \mu_B$ ($x = 0.1$ and 0.15) at 2 K. It is suggested that ferromagnetism is originated predominantly from the $\text{Mn}^{3+}\text{--O--Mn}^{3+}$ and $\text{Mn}^{3+}\text{--O--Mn}^{4+}$ superexchange interactions whereas bond angles fluctuation leads to magnetic frustrations. Enhancement of covalence slightly increases ferromagnetism.

DOI: [10.12693/APhysPolA.132.240](https://doi.org/10.12693/APhysPolA.132.240)

PACS/topics: 61.05.fm, 68.37.Hk, 71.70.Ej, 75.30.Et

1. Introduction

Mixed-valence manganese and cobalt perovskites such as $\text{La}_{1-x}\text{Sr}_x\text{Mn}(\text{Co})\text{O}_3$ with charge, orbital, spin, and lattice degrees of freedom, have attracted great attention [1]. The interplay between ferromagnetism and electroconductivity in these compounds has been explained using the double exchange model [2]. This model suggests real electron transfer from $\text{Mn}^{3+}(\text{Co}^{3+})$ to $\text{Mn}^{4+}(\text{Co}^{4+})$ while this mechanism is effective only for the mixed-valence systems. However, it was found that the ferromagnetic state can be stabilized in some compounds where manganese or cobalt ions are in 3+ or 4+ oxidation state only [3–11]. Orbitaly disordered state in parent LaMnO_3 above 750 K results in dominant ferromagnetic interactions, as confirmed by the positive Weiss constant ($\theta \approx 160$ K [3, 4]). Orbital ordering leads to anisotropic superexchange interactions and A-type antiferromagnetic order below 140 K [3]. The long-range ferromagnetic component has been observed in the $\text{LaMn}_{1-x}\text{Ga}_x\text{O}_3$ ($0.2 < x < 0.6$) and $\text{LaMn}_{1-x}\text{Cr}_x\text{O}_3$ ($0.4 < x < 0.6$) series containing only Mn^{3+} species [5–11]. These series show gradual transition into the orbitaly disordered state upon substitution with Ga^{3+} ($x > 0.5$) or Cr^{3+} ($x > 0.35$) ions. The manganese substitution is accompanied by an increase in ferromagnetic component. It was found that the homovalent $\text{LaCo}^{3+}\text{O}_3$ and $\text{SrCo}^{4+}\text{O}_3$ cobaltites can be ferromag-

netic with $T_C = 90$ K (LaCoO_3) [12] and $T_C = 305$ K (SrCoO_3) [13]. Insulating ferromagnetic state was also observed in orbitaly disordered $\text{La}_{0.7}\text{Sr}_{0.3}\text{Mn}_{0.85}\text{Nb}_{0.15}\text{O}_3$ and $\text{La}_{0.7}\text{Sr}_{0.3}\text{Mn}_{0.85}\text{Sb}_{0.15}\text{O}_3$ where manganese ions are in the 3+ homovalent state [14, 15].

According to the neutron powder diffraction (NPD) data [6] the orbitaly ordered $\text{LaMn}_{0.5}\text{Ga}_{0.5}\text{O}_3$ is a homogeneous collinear ferromagnet [6]. It was proposed that the ferromagnetism in the orbitaly ordered state of the homovalent manganite can be caused by orbital fluctuations [3, 5, 9]. According to this approach, substitution of trivalent manganese ions by gallium results in decrease of static Jahn–Teller distortion and strengthens the ferromagnetic component of the superexchange interactions. Therefore it has been suggested that ferromagnetism can occur in the homogeneous d_{z^2} -orbitaly ordered phase by mixing of e_g -orbitals with different symmetry, while orbital disorder can lead to frustration of magnetic interactions [7, 12].

On the other hand, ferromagnetism is much stronger in the orbitaly disordered phases, e.g. $\text{LaMn}_{1-x}\text{Ga}_x\text{O}_3$ ($x = 0.6$) and $\text{LaMn}_{1-x}\text{Cr}_x\text{O}_3$ ($0.35 < x < 0.6$) [6, 10]. Using dynamic magnetization measurements it was shown that $\text{LaMn}_{0.5}\text{Ga}_{0.5}\text{O}_3$ is not a homogeneous ferromagnet as it was suggested earlier [7]. Note that the superexchange interactions $\text{Mn}^{3+}\text{--O--Mn}^{4+}$ can be strongly ferromagnetic, similarly to the double exchange mechanism [9]. One can conclude that the situation with magnetic interactions in both the homo- and heterovalent manganites (cobaltites) has not been fully understood so far.

It is well known that the optimally doped $\text{La}_{0.7}\text{Sr}_{0.3}(\text{Mn}_{0.7}^{3+}\text{Mn}_{0.3}^{4+})\text{O}_3$ has the highest Curie

*corresponding author; e-mail: troyan@physics.by

point ($T_C = 390$ K) of the mixed-valence manganites. Substitution of all Mn^{4+} ions by Ti^{4+} leads to formation of homovalent manganese (Mn^{3+}) ions whereas substitution of Ti^{4+} by Al^{3+} introduces Mn^{4+} ions proportionally to the chemical doping level.

In this paper the structure and magnetic properties of manganites heavily doped with Ti^{4+} and Al^{3+} ions are discussed.

2. Experimental procedures

Ceramic samples of $La_{0.7}Sr_{0.3}Mn_{0.7}Ti_{0.3-x}Al_xO_3$ ($0 \leq x \leq 0.15$) series were prepared by a solid-state reaction technique using high purity oxides La_2O_3 , Mn_2O_3 , TiO_2 , Al_2O_3 and carbonate $SrCO_3$ taken in a stoichiometric ratio and thoroughly mixed in a planetary mill (Retsch, 300 rpm, 30 min). La_2O_3 was preliminary annealed at $1100^\circ C$ in air in order to remove moisture. The synthesis was performed at 1450 – $1580^\circ C$ for 7 h in air, using a two-step procedure with an interim annealing at $1200^\circ C$ for 5 h followed by thorough grinding. The samples were cooled from the synthesis temperature down to $300^\circ C$ with a rate of $300^\circ C/h$. X-ray diffraction (XRD) patterns were recorded using the DRON-3M diffractometer with $Cu K_\alpha$ radiation. The scanning electron microscope LEO 1455 VP was used to study the microstructure. To determine the elemental composition of the samples X-ray microanalysis was conducted using the energy dispersive X-ray spectroscopy microanalyzer Aztec Energy Advanced X-Max 80 (EDX). NPD measurements were performed for the $x = 0, 0.1, 0.15$ compounds using the high resolution powder diffractometer E9 (FIREPOD) with $\lambda = 1.7982 \text{ \AA}$ at the Helmholtz-Zentrum for Materials and Energy, Berlin. The Rietveld refinement of the collected data has been performed using the FULLPROF software package [16]. Magnetic properties of the samples were investigated using PPMS set-up (Cryogenic Ltd.) in the magnetic fields up to 14 T and in the temperature range 5–320 K.

3. Results and discussion

The XRD data collected at room temperature for all the samples show a single phase structure without any detectable impurities. Diffraction peaks for all the samples can be indexed within the rhombohedral unit cell (space group $R\bar{3}c$). Substitution of Ti^{4+} by Al^{3+} or Ge^{4+} leads to decrease of unit cell volume.

Shape and size of the ceramic samples particles were examined using the scanning electron microscope (SEM) LEO 1455 VP. The decrease of the synthesis time and the titanium content leads to a decrease in grain size (Fig. 1). The investigations of the composition of synthesized samples by registration of element distribution along any given line on the surface have shown a good accordance with the prescribed parameters. There is an insignificant variation of the observed La, Sr, Mn, Ti and Al contents in different crystallites so the sample can be regarded as practically homogeneous in composition.

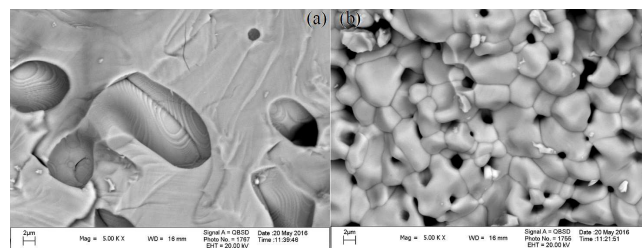


Fig. 1. SEM image of $La_{0.7}Sr_{0.3}Mn_{0.7}Ti_{0.2}Al_{0.1}O_3$ ($T_{sint} = 1480^\circ C$, 7 h) (a) and $La_{0.7}Sr_{0.3}Mn_{0.7}Ti_{0.1}Al_{0.2}O_3$ ($T_{sint} = 1560^\circ C$, 4 h) (b).

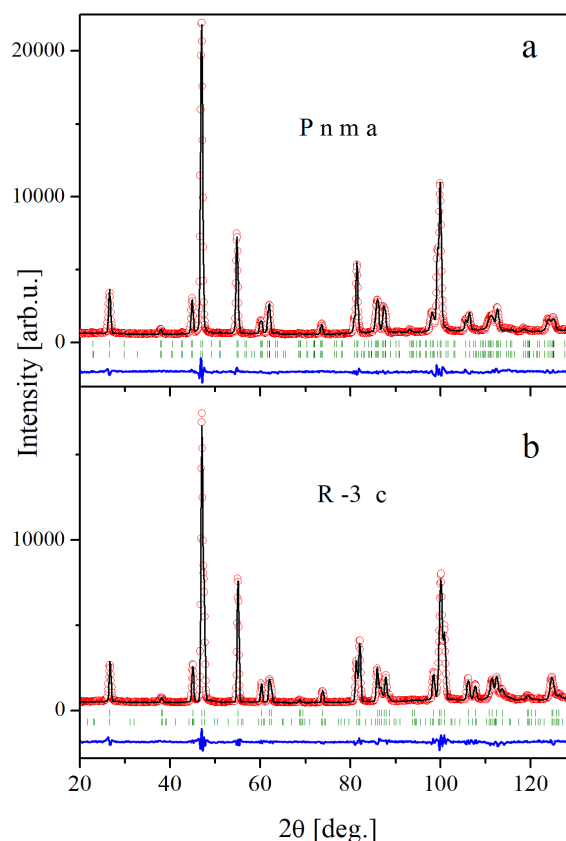


Fig. 2. Observed (circles), calculated (solid line) and difference patterns resulting from the Rietveld analysis of the NPD data of $La_{0.7}Sr_{0.3}Mn_{0.7}Ti_{0.3}O_3$ (a) and $La_{0.7}Sr_{0.3}Mn_{0.7}Ti_{0.2}Al_{0.1}O_3$ (b) at 2 K.

The NPD patterns for the $La_{0.7}Sr_{0.3}Mn_{0.7}Ti_{0.3-x}Al_xO_3$ compounds were obtained in the temperature range 2–300 K. The NPD patterns at 2 K recorded for $x = 0$ and $x = 0.15$ are shown in Fig. 2. At room temperature the diffraction peaks for $La_{0.7}Sr_{0.3}Mn_{0.7}Ti_{0.3}O_3$ can be indexed within the rhombohedral unit cell (space group $R\bar{3}c$). However, with the temperature decrease down to 150 K there is a structural phase transition into the orthorhombic phase (space group $Pnma$). The structural transition is not associated with magnetic ordering. Magnetization

starts to develop below 80 K, while the sample is paramagnetic at 150 K according to both the NPD and magnetization data (Fig. 2). The ratio between the unit cell parameters at 2 K ($c > a \approx b/\sqrt{2}$) corresponds to the orbitally disordered phase in accordance with the Goodenough consideration [7]. The crystal structures of both $\text{La}_{0.7}\text{Sr}_{0.3}\text{Mn}_{0.7}\text{Ti}_{0.2}\text{Al}_{0.1}\text{O}_3$ and $\text{La}_{0.7}\text{Sr}_{0.3}\text{Mn}_{0.7}\text{Ti}_{0.15}\text{Al}_{0.15}\text{O}_3$ in the temperature range 2–300 K were successfully refined within the rhombohedral space group $R\bar{3}c$. The magnetic contributions into the diffraction peaks (020), (101), (002), (121), (200) were observed at 2 K for all the samples. This means that the magnetic structure should be described as ferromagnetic. The refined structural and magnetic parameters at 2 K and 300 K are presented in Table I. The substitution of Ti^{4+} by Al^{3+} is accompanied by a gradual increase of the bond angle Mn–O–Mn which leads to enhancement of the covalent component of chemical bond. Decrease in the distance Mn–O also favours covalency increase. The magnetic moments per manganese ion evaluated from the NPD data are found to be around $1.3 \mu_B$ ($x = 0$) and $1.7 \mu_B$ ($x = 0.1$ and 0.15) at 2 K.

TABLE I

Crystal and magnetic structure parameters deduced from the Rietveld refinement of $\text{La}_{0.7}\text{Sr}_{0.3}\text{Mn}_{0.7}\text{Ti}_{0.3-x}\text{Al}_x\text{O}_3$ NPD patterns.

x	0		0.1		0.15	
	2	300	2	300	2	300
T [K]						
SG	$Pnma$	$R-3c$	$R-3c$	$R-3c$	$R-3c$	$R-3c$
a [Å]	5.497	5.538	5.513	5.519	5.501	5.506
b [Å]	7.774	5.538	5.513	5.519	5.501	5.506
c [Å]	5.539	13.426	13.354	13.394	13.329	13.368
V [Å ³]	236.73	356.55	351.51	353.20	349.26	350.93
V_p [Å ³]	59.18	59.43	58.58	58.87	58.21	58.49
Mn–O1 [Å]	1.971	1.968	1.958	1.960	1.953	1.955
Mn–O2 [Å]	1.990/1.942					
Mn–O1–Mn [°]	160.87	164.9	164.9	165.7	165.6	166.3
Mn–O2–Mn [°]	165.95					
Mn ⁴⁺ [%]	0		14.3		21.4	
M [μ_B]	1.3		1.7		1.7	
χ^2	2.96	4.37	3.45	2.12	4.66	2.62
R_p [%]	3.99	4.31	4.73	3.26	4.78	3.05
R_{wp} [%]	5.17	5.72	6.11	4.28	6.44	4.01
R_B [%]	4.86	3.37	4.82	4.19	4.74	4.80

The temperature dependences of magnetization for $\text{La}_{0.7}\text{Sr}_{0.3}\text{Mn}_{0.7}\text{Ti}_{0.3-x}\text{Al}_x\text{O}_3$ and $\text{La}_{0.7}\text{Sr}_{0.3}\text{Mn}_{0.7}\text{Ti}_{0.2}\text{Ge}_{0.1}\text{O}_3$ measured in a small magnetic field are presented in Fig. 3. The compound formally free of Mn^{4+} ions ($x = 0$) does not exhibit a pronounced anomaly associated with T_C on the temperature dependence of magnetization thus possibly indicating magnetic inhomogeneity. The $\text{La}_{0.7}\text{Sr}_{0.3}\text{Mn}_{0.7}\text{Ti}_{0.2}\text{Ge}_{0.1}\text{O}_3$ compound does not contain Mn^{4+} ions either. However, the Ge-containing compound exhibits much stronger magnetization and there

is a pronounced magnetization maximum on the field cooling (FC) curve around 35 K (Fig. 3). One can see that substitution of Ti^{4+} ions by Al^{3+} ones results in the increase of the Curie temperature which is maximal for $\text{La}_{0.7}\text{Sr}_{0.3}\text{Mn}_{0.7}\text{Ti}_{0.15}\text{Al}_{0.15}\text{O}_3$ (formal content of Mn^{4+} is about 21%). The $x = 0.1$ compound has very close T_C (Fig. 3). Magnetization starts to develop slightly below 100 K for both $x = 0.1$ and $x = 0.15$ compounds. There is a maximum of magnetization which is observed on the FC curve around 35–40 K (Fig. 3). These data show that the Mn^{4+} content is not the unique factor controlling ferromagnetism.

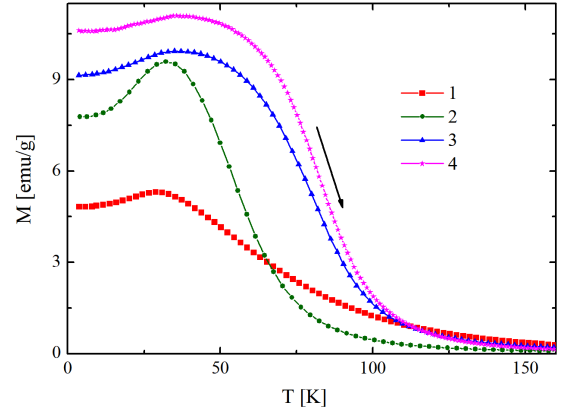


Fig. 3. FC magnetization as a function of temperature for $\text{La}_{0.7}\text{Sr}_{0.3}\text{Mn}_{0.7}\text{XO}_3$ compounds in a field of 0.02 T. X = $\text{Ti}_{0.3}$ (1), $\text{Ti}_{0.2}\text{Ge}_{0.1}$ (2), $\text{Ti}_{0.2}\text{Al}_{0.1}$ (3), $\text{Ti}_{0.15}\text{Al}_{0.15}$ (4).

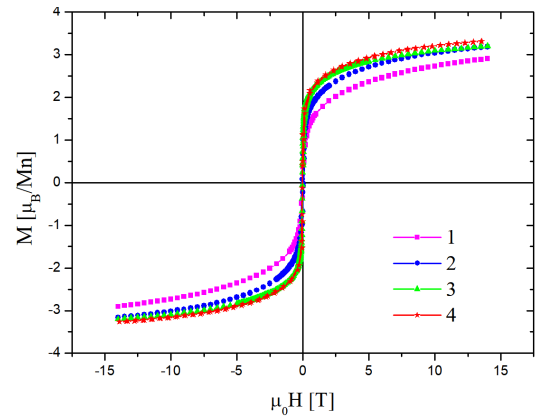


Fig. 4. Magnetic moments as a function of magnetic field obtained for $\text{La}_{0.7}\text{Sr}_{0.3}\text{Mn}_{0.7}\text{XO}_3$ at 5 K. X = $\text{Ti}_{0.3}$ (1), $\text{Ti}_{0.2}\text{Ge}_{0.1}$ (2), $\text{Ti}_{0.2}\text{Al}_{0.1}$ (3), $\text{Ti}_{0.15}\text{Al}_{0.15}$ (4).

Magnetization dependences as a function of magnetic field measured at 5 K are shown in Fig. 4. The evolution of a ferromagnetic component upon increasing Al-doping is clearly evident. For the composition $x = 0.15$ spontaneous magnetization is larger than that for $x = 0$ but very

close to that obtained for $x = 0.1$ compound. Magnetization of the composition $\text{La}_{0.7}\text{Sr}_{0.3}\text{Mn}_{0.7}\text{Ti}_{0.2}\text{Ge}_{0.1}\text{O}_3$ is significantly larger than that obtained for the compound doped only by Ti^{4+} ions. Magnetic moments per manganese ion evaluated from the magnetization data approximated to $H = 0$ are around $1.3 \mu_B$ ($x = 0$) and $1.7 \mu_B$ ($x = 0.15$).

The determined structural parameters evidence that the orthorhombic distortion of the crystal lattice as found at low temperatures for the $\text{La}_{0.7}\text{Sr}_{0.3}\text{Mn}_{0.7}\text{Ti}_{0.3}\text{O}_3$ composition is not caused by long-range orbital ordering. The unit cell parameters correspond to the orbitally disordered O-type phase (Table I). Apparently the orthorhombic distortion is caused by steric effects similar to the case of optimally doped $\text{La}_{1-x}\text{Ca}_x\text{MnO}_3$, where the O-type of the orthorhombic distortion also points out to the orbitally disordered state. Hence the small ferromagnetic component is not associated with orbital ordering.

In the $\text{La}_{0.7}\text{Sr}_{0.3}\text{Mn}_{0.7}\text{Ti}_{0.3-x}\text{Al}_x\text{O}_3$ compounds there is slight enhancement of ferromagnetism upon doping with $\text{Al}^{3+}(\text{Mn}^{4+})$ doping. Ferromagnetism can be explained by positive superexchange interactions associated with virtual excitations of e_g electrons in the orbital of neighbouring Mn^{3+} and Mn^{4+} ions or double exchange mechanism through direct electron transfer between Mn^{3+} and Mn^{4+} ions. Apparently both mechanisms affect the magnetic state. Let us consider the argument that the superexchange interaction mechanism is a predominant one. The substitution of Ti^{4+} by Ge^{4+} ions does not change manganese valence but enhances the covalency because Ge^{4+} ions have the ionic radius much smaller than that of Ti^{4+} . This leads to decrease of the Mn–O distances. The formally Mn^{4+} free compound $\text{La}_{0.7}\text{Sr}_{0.3}\text{Mn}_{0.7}\text{Ti}_{0.2}\text{Ge}_{0.1}\text{O}_3$ exhibits a pronounced magnetic transition: magnetization starts to develop around 60 K. The Curie temperature of the $\text{La}_{0.7}\text{Sr}_{0.3}\text{Mn}_{0.7}\text{Ti}_{0.3-x}\text{Al}_x\text{O}_3$ ($x = 0.1$ and $x = 0.15$) compounds is higher: magnetization starts to develop below 90 K, magnetization becomes larger than that for $x = 0$ compounds and is comparable with the value close to that observed for the compounds doped by Ti/Ge ions. Also the magnetization of these compounds is increased up to $1.7 \mu_B$ ($x = 0.1$), and then ($x > 0.1$) remains at the same level.

According to the neutron diffraction studies the crystal structure of other $\text{Ti}^{4+}/\text{Al}^{3+}$ substituted manganites is characterized by the rhombohedral space group $R\bar{3}c$ in the temperature range 5–300 K. The substitution of Ti^{4+} by Al^{3+} ions causes a contraction of the unit cell volume that mainly increases the Mn–O–Mn bond angle and decreases the Mn–O distance (Table I). The increase of Mn–O–Mn angle enhances the ferromagnetic interaction, and decreases the contribution of antiferromagnetic interactions. It is well known that the Mn–O–Mn angle controls $3d(\text{Mn})-2p(\text{O})$ hybridization in manganites with the perovskite-like structure [17, 18]. On the other hand, structural disorder can decrease the covalency because of local variations of the bond angle Mn–

O–Mn. There is a critical value of the Mn–O–Mn angle associated with a change in the sign of the superexchange interaction from positive to negative [17, 18]. Apparently local fluctuations of the bond angle Mn–O–Mn result in the inhomogeneous magnetic state of these compounds and stabilize antiferromagnetic clusters formed in the ferromagnetic matrix at low temperature.

4. Conclusions

We have studied the $\text{Ti}^{4+}/\text{Al}^{3+}$ substituted $\text{La}_{0.7}\text{Sr}_{0.3}\text{MnO}_3$ manganites where formal concentration of Mn^{4+} ions increases from 0% up to 21% upon Al^{3+} doping. It is shown that the compounds include ferromagnetic components with the magnetic moments around $1.3 \mu_B$ ($x = 0$) and $1.7 \mu_B$ ($x = 0.1$ and 0.15) at 2 K. The composition $x = 0$ undergoes structural transformation upon cooling from the rhombohedral symmetry (space group $R\bar{3}c$) to the orthorhombic one (space group $Pnma$). This transition occurs around 150 K whereas the temperature of magnetic ordering is below 80 K. The structural refinement shows that all the compositions are orbitally disordered down to 2 K. The substitution of Ti^{4+} by Al^{3+} is accompanied by a gradual increase of the bond angle Mn–O–Mn and decrease of Mn–O distance which leads to enhancement of the covalent component of the chemical bond. It is suggested that ferromagnetism predominantly originates from the superexchange interactions via oxygen due to a large covalent component of the chemical bond.

The obtained results can be used in the preparation and explanation of physicochemical properties of new oxide materials with the perovskite structure. The new materials based on magnetoresistive manganite perovskite will be used in the development of new information storage devices, and processing and creation of sensors, sensitive to changes in magnetic parameters.

Acknowledgments

This work is supported by the Belarusian Republican Foundation for Fundamental Research (project F15SO-008).

References

- [1] E. Dagotto, T. Hotta, A. Moreo, *Phys. Rep.* **344**, 1 (2001).
- [2] C. Zener, *Phys. Rev.* **82**, 403 (1951).
- [3] J.S. Zhou, J.B. Goodenough, *Phys. Rev. B* **60**, R15002 (1999).
- [4] A. Trokiner, S. Verkhovskii, A. Gerashenko, Z. Volkova, O. Anikeenok, K. Mikhalev, M. Eremin, L. Pinsard-Gaudart, *Phys. Rev. B* **87**, 125142 (2013).
- [5] J.S. Zhou, H.Q. Yin, J.B. Goodenough, *Phys. Rev. B* **63**, 184423 (2001).
- [6] J. Blasco, J. Garcia, J. Campo, M.C. Sanchez, G. Subias, *Phys. Rev. B* **66**, 174431 (2002).

- [7] J.S. Zhou, Y. Uwatoko, K. Matsubayashi, J.B. Goodenough, *Phys. Rev. B* **78**, 220402 (2008).
- [8] D. Rinaldi, R. Caciuffo, J.J. Neumeier, D. Fiorani, S.B. Oseroff, *J. Magn. Magn. Mater* **272-276**, E571 (2004).
- [9] J.B. Goodenough, *Magnetism and the Chemical Bond*, Interscience, New York 1963.
- [10] J. Deisenhofer, M. Paraskevopoulos, H.-A. Krug von Nidda, A. Loidl, *Phys. Rev. B* **66**, 054414 (2002).
- [11] A.Y. Ramos, H.C.N. Tolentino, M.M. Soares, S. Grenier, O. Bunău, Y. Joly, F. Baudalet, F. Wilhelm, A. Rogalev, R.A. Souza, N.M. Souza-Neto, O. Proux, D. Testemale, A. Caneiro, *Phys. Rev. B* **87**, 220404 (2013).
- [12] J.-Q. Yan, J.-S. Zhou, J.B. Goodenough, *Phys. Rev. B* **70**, 014402 (2004).
- [13] Y. Long, Y. Kaneko, S. Ishiwata, Y. Taguchi, Y. Tokura, *J. Phys. Condens. Matter* **23**, 245601 (2011).
- [14] I.O. Troyanchuk, D. Karpinsky, V. Efimov, V. Sikolenko, O. Prokhnenko, M. Bartkowiak, *J. Phys. Condens. Matter* **26**, 396002 (2014).
- [15] I.O. Troyanchuk, M.V. Bushinsky, V. Sikolenko, V. Efimov, N.V. Volkov, D.M. Többens, C. Ritter, B. Raveau, *J. Alloys Comp.* **619**, 719 (2015).
- [16] T. Roisnel, J. Rodriguez-Carvajal, *Mater. Sci. Forum* **378-381**, 118 (2001).
- [17] J.S. Zhou, J.B. Goodenough, *Phys. Rev. B* **68**, 144406 (2003).
- [18] B. Dabrowski, J. Mais, S. Kolesnik, O. Chmaissem, *J. Phys. Conf. Ser.* **303**, 012057 (2011).